

INTERFERENCE REJECTION FOR SONARS VIA LOW COMPLEXITY ADAPTIVE BEAMFORMING

TIB Lønmo Kongsberg Maritime AS, Horten, Norway and University of Oslo, Oslo, Norway
A Austeng University of Oslo, Oslo, Norway.
RE Hansen Norwegian Defence Research Establishment (FFI), Kjeller, Norway
and University of Oslo, Oslo, Norway

1 INTRODUCTION

Accurate mapping of the seabed using active high frequency sonar is of importance in many applications, for example in inspection of underwater infrastructure and environmental seabed mapping. The delay-and-sum (DAS) beamformer is commonly used for beamforming. However, it suffers from high sidelobes, which make it susceptible to masking of weak signals when there are strong, interfering, signals present. This may cause serious problems, as low quality data, loss of data and range reduction.

Conventional aperture shading is used to mitigate this, with a trade-off against resolution. By adjusting the beampattern in real time, adaptive methods promise to provide increased sidelobe suppression while keeping or improving the resolution. This is done by adjusting the beam pattern to have low gain in the directions with interference and allowing large sidelobes in directions without signal.

In this work, we investigate the interference rejection capabilities of the Low Complexity Adaptive (LCA) beamformer, which is a computationally cheap version of the Minimum Variance Distortionless Response (MVDR) beamformer. It uses a discrete search space and bases its decision on a single sample. The discrete search space also make LCA resistant to signal suppression, which is a serious issue for MVDR in active applications.

In earlier work, we have shown that LCA outperform the DAS beamformers for simulated and measured data over a flat seafloor¹. This time we test LCA further by applying it to data collected by a high-resolution echosounder over the wreck of an oil tanker. The wreck has sharp edges and big differences in backscatter level, which is common challenges for the DAS beamformer. We investigate how LCA performs compared to the unweighted and a weighted DAS beamformer.

2 LOW COMPLEXITY ADAPTIVE BEAMFORMING

The adaptive Minimum Variance Distortionless Response (MVDR) beamformer minimizes the variance of the beamformer output while passing signals from the steering direction through undistorted². It often needs to use diagonal loading and spatial smoothing to make it robust against errors in estimation of the covariance matrix and coherent signals. This reduces the resolution of the beamformer³. Solving for the MVDR weights also require inversion of the sample covariance matrix, which make the method too computationally expensive for some applications.

Low Complexity Adaptive (LCA) beamforming⁴ uses the same optimization criteria but a discrete search space consisting of a predefined set of weights. In practice this means that we apply ordinary delay-and-sum beamforming for all weights and choose the minimum beam value. The discrete search space let LCA avoid the need to estimate and invert the covariance matrix. It also eliminates the need for spatial smoothing and diagonal loading, since the method does not have enough freedom to create signal suppression. The computational complexity for LCA is therefore of order $N_{\text{El}}N_w$ instead of N_{El}^3 , where N_{El} is the number of elements and N_w is the number of weights in the LCA weight set. This means that it is significantly faster and may perform better than MVDR^{5,6}.

MVDR use a variety of effects to achieve its good results. We have chosen a weight set for LCA that

captures the most important effects. MVDR can for example use an asymmetric mainlobe, which gives sharper edges, and low sidelobes in regions with strong signals⁴. Our set consists of the following ten weights: uniform, kaiser with $\beta = 2, 3, 4$, and kaiser with $\beta = 3$ steered to $1/2, 3/4$, and 1 times the distance to first zero of the uniform window (in both directions). This is a subset of the weight set from Synnevåg et al.⁴, we excluded two weights since they seemed to reduce the performance. All weights are normalized such that the sum of the weight equals one, to satisfy the distortionless constraint.

3 DATA COLLECTION AND PROCESSING

We collected data with a high-resolution seabed mapping echosounder over the wreck of an oil tanker called Holmengraa, located outside Horten, Norway. Holmengraa was a Norwegian 1500 dwt oil tanker. Allied airplanes sank it in 1944, while it was sailing under a German flag. The wreck is approximately 68 meters long and 9 meters wide, and lies in a slope at almost 80 meters depth. Figure 1 show an interferometric SAS image of the wreck. The wreck has common challenging features as small and strong scatterers and sharp edges.

Our data were collected using a high-resolution seabed mapping echosounder. The echosounder use a Mill's cross setup⁷ with two linear arrays: A transmitter with .5 degree opening along-track and a receiver with 1 degree opening angle across-track (for the used frequency). A tapered 285 kHz single frequency pulse was used. The data were collected on a calm and sunny day, without any rain or significant wind or waves.

For each channel in the received data, we do bandpass and matched filtering. Then we steer toward the wanted angle via time delay and do beamforming and bottom detection on the results. Later in this paper we compare different beamforming methods. The beamforming is then the only step to be changed, all the other processing steps stay the same.

Our processing is somewhat simplified since it assumes a homogeneous ocean and that all vessel movement is along track (no motion stabilization). Because of the calm data collection day and near vertical beams we expect these inaccuracies to be small and that they will not affect the conclusions from this study.

We do bottom detection via the maximum amplitude instant method, commonly used near vertical incidence⁷. The technique use the maximum amplitude instant as the arrival time for the bottom echo. Using this instant, combined with beam direction and propagation speed, we can calculate the bottom location.

4 RESULTS AND DISCUSSION

We applied uniformly weighted (or unweighted) DAS, kaiser ($\beta = 3$) weighted DAS, and LCA beamforming to the echosounder data across Holmengraa. Unweighted and kaiser weighted DAS are selected to give two versions of the resolution-sidelobe tradeoff. Uniform DAS give good resolution at the cost of high sidelobes, while kaiser DAS ($\beta = 3$) gives medium sidelobe level (24 dB) and reduced resolution.

Figure 2 show all detections across Holmengraa for the three methods. We have calculated beams for every 0.3 degrees. This is approximately a factor 3 oversampling, which we have done since adaptive methods can achieve higher resolution than conventional methods.

The most apparent difference between the plots is that uniform weighted DAS have some outliers. Apart from the plots are very similar, but the keen eye may see a couple outliers for LCA that are not present for kaiser DAS. To explain the outliers and look closer on other effects we will examine three pings, shown in Figure 3, Figure 4 and Figure 5, in detail.

Figure 3 show a case with very strong backscatter from some areas. This give strong sidelobes for the uniform DAS beamformer, visible as light blue arcs at certain ranges. The sidelobes are stronger than the bottom echoes in this case, which cause misdetections and outliers in Figure 2. The distant

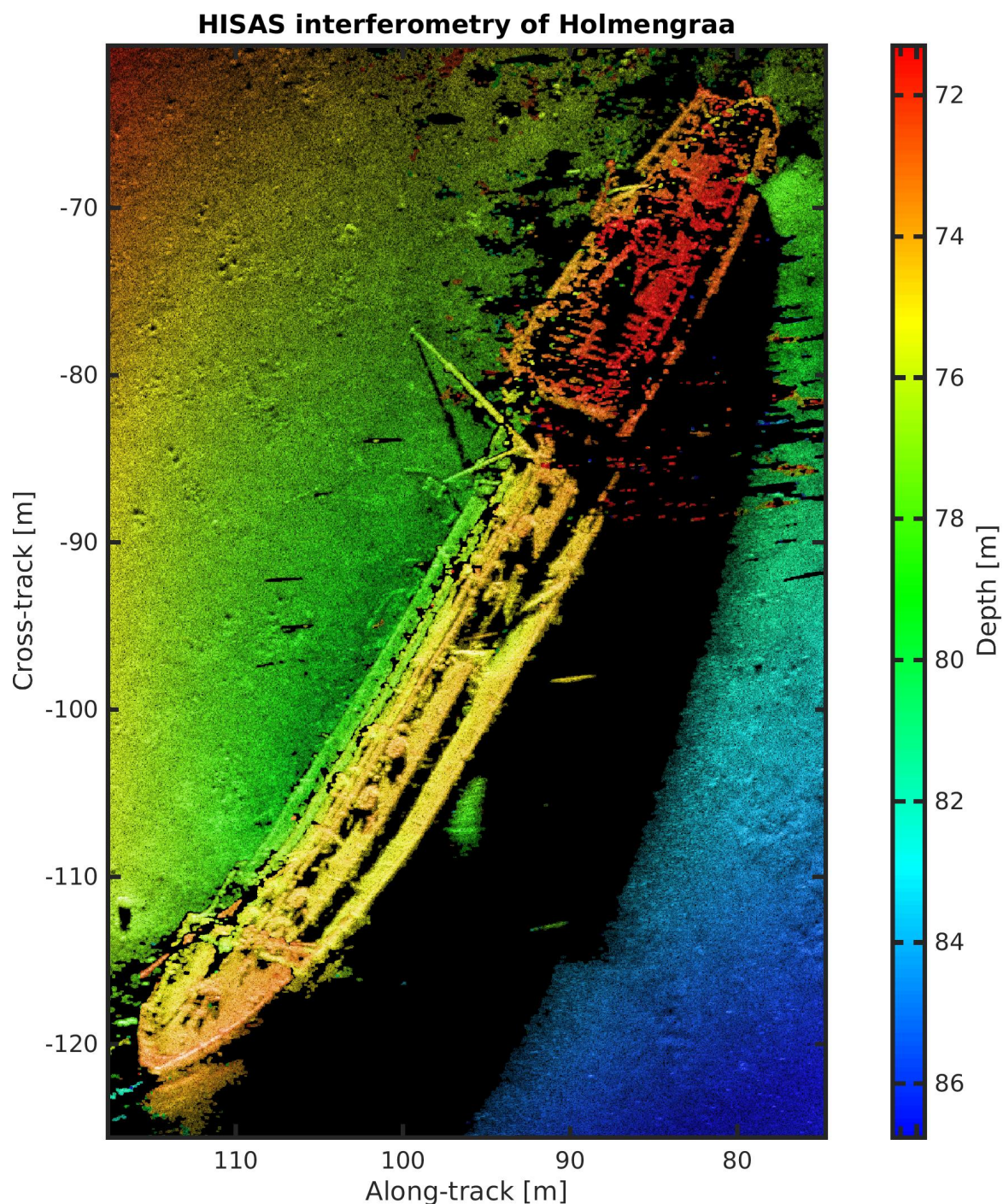


Figure 1: Interferometric SAS image of Holmengraa. Image by the Norwegian Defence Research Establishment (FFI).

misdetectors are easy to identify, but it the ones close to the right side of the wreck may be hard to identify.

By applying kaiser weighted beamforming we greatly reduce these sidelobes and consequently remove these misdetections. However, the widened mainlobe smear out the details and miss other features. For example, the hole at around 5 meters across track distance, that were picked up by the uniform beamformer, is lost by the kaiser beamformer.

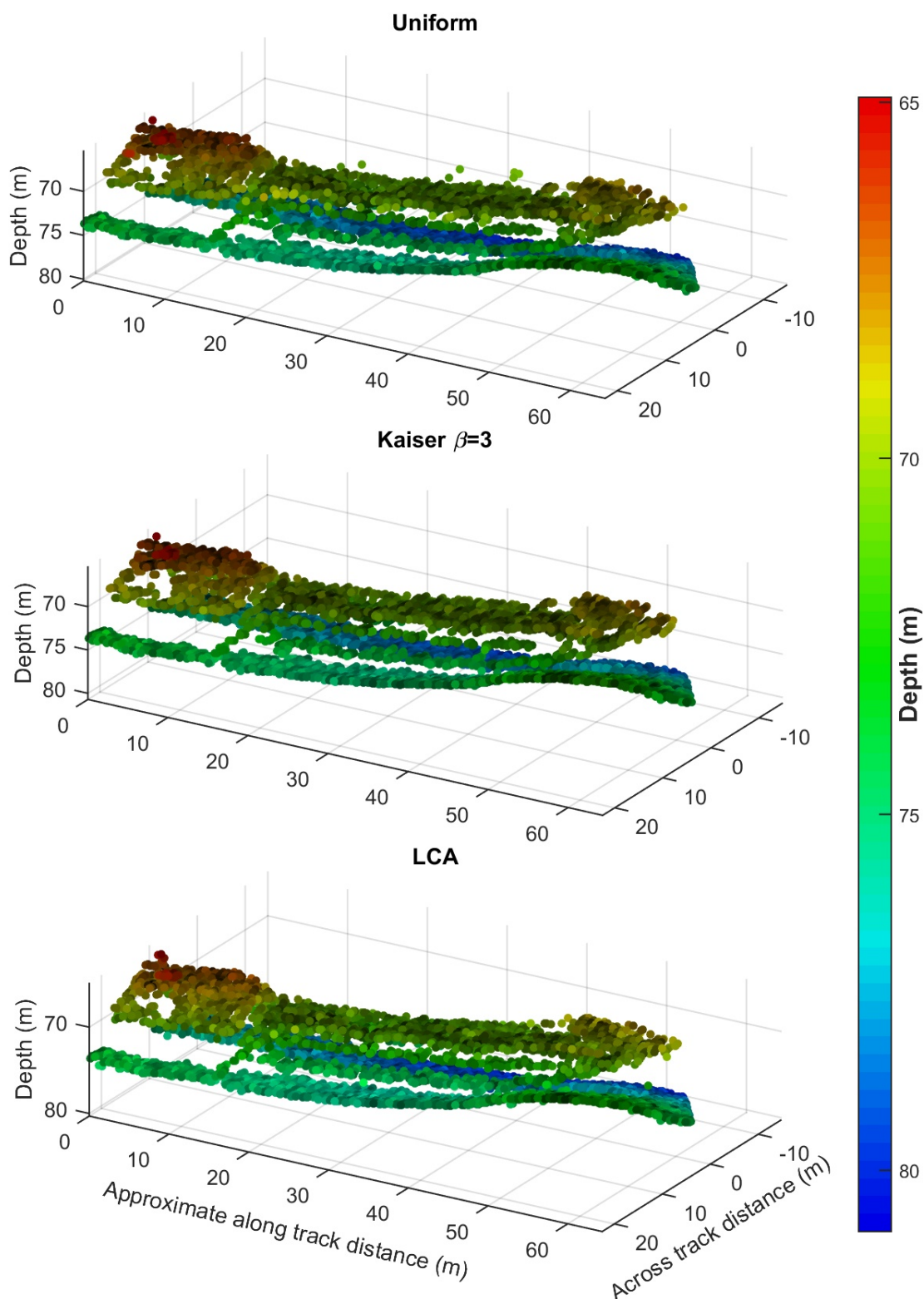


Figure 2: Scatterplot of amplitude detections from whole swath. Color indicate depth, brightness beam level for detections instant. The along track distance has been approximated by moving each line according to the mean ping rate and vessel speed. Note that the average depth differ from Figure 1. This may be due to lack of tidal correction and/or transducer depth correction. Axis labels are the same in all three plots.

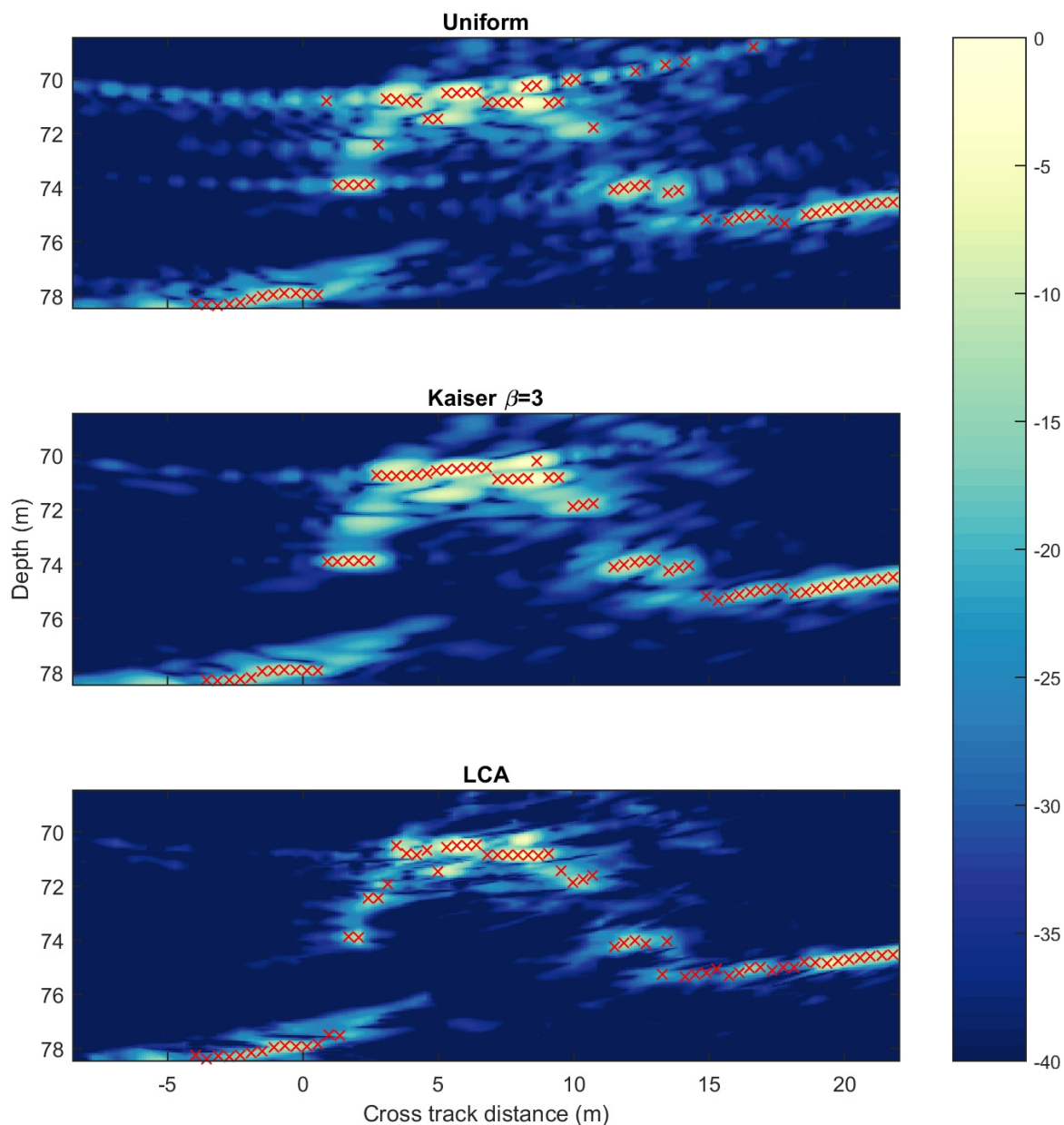


Figure 3: Beam power and bottom detections for different beamforming techniques on measured data, ping 33. Red crosses are amplitude detections. The colormap represent normalized beam power in dB. The strongest beam sample across the three beams is set to 0 dB.

When using LCA we can get the best of both worlds. We get good sidelobe suppression, better than for the kaiser weighted DAS, while picking up the hole. LCA also get significantly smaller extension, even when compared to uniform DAS, of what appears to be small sources at 2 meters across track distance and slightly above deck at 8 meters cross track distance (no detection on the latter for LCA). This enables the LCA detections to provide a better contour for the left side of the ship.

We see the same effects in figure 4. There are strong sidelobe arcs for the uniform beams, which are lower or nonexistent for the kaiser and LCA beams. LCA seem to be able to resolve more detail. Localized scatterers as the one to the top left of the deck have smaller extent for LCA. The LCA detections also give an more likely right edge for the wreck, while uniform and kaiser weighted DAS seem to be dominated by strong points in neighbor beams.

On the bottom to the left LCA seem to give a more probable shape for the seabottom than the other

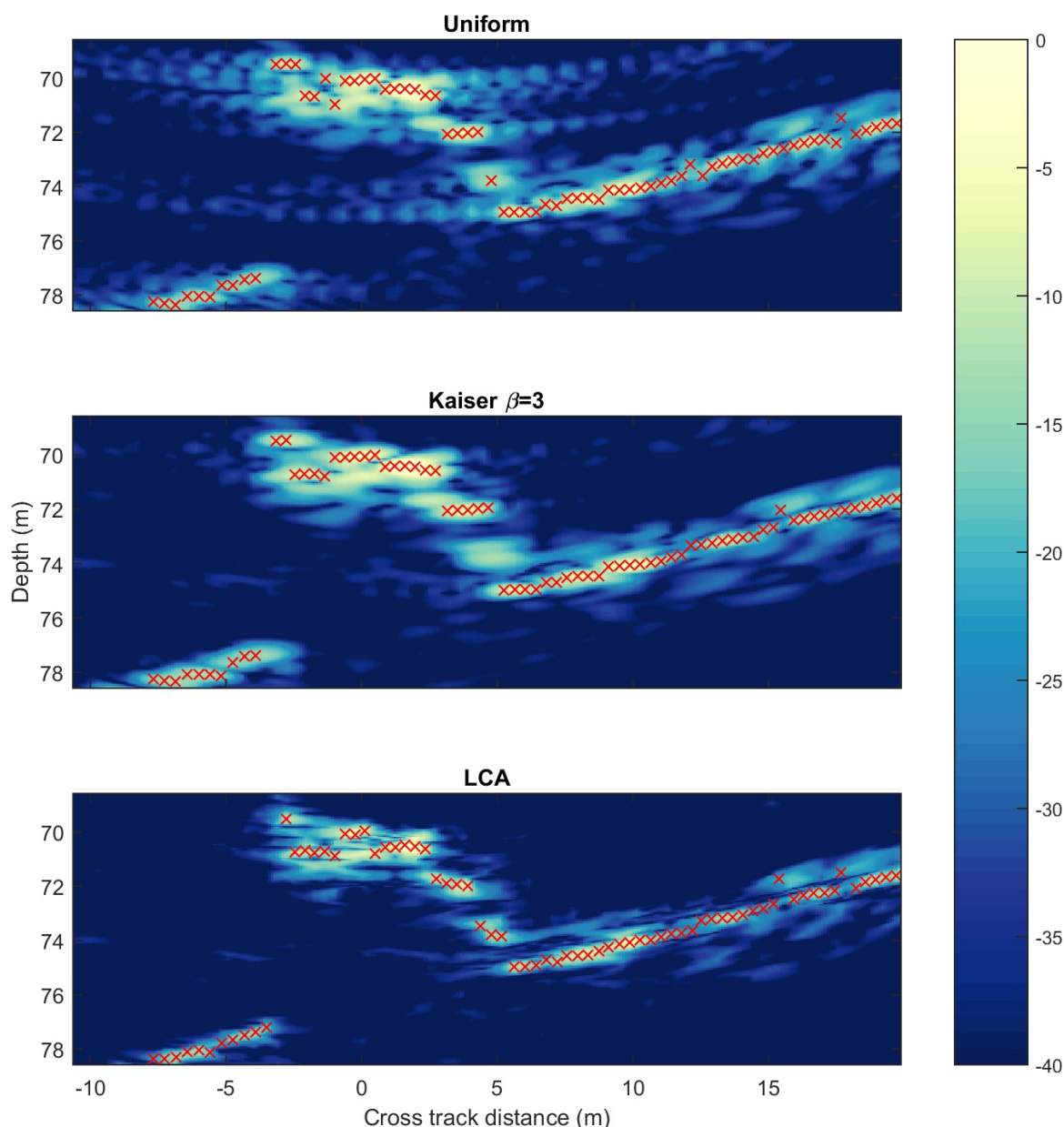


Figure 4: Beam power and bottom detections for different beamforming techniques on measured data, ping 74. Red crosses are amplitude detections. The colormap represent normalized beam power in dB. The strongest beam sample across the three beams is set to 0 dB.

methods. The uniform and kaiser detections seem lie in groups at constant range, indicating that neighbor beams are dominated by a strong center beam. To the far right we see a few outliers for LCA, more than for the kaiser weighted beams. The next figure has a clearer example of this.

Figure 5 shows an example were LCA seem to perform worse. At 15 meters cross track distance we see a two meter vertical spread in the LCA detections while the uniform detections follow a straight line. A few of the kaiser detections are a meter above the line, which seem to be bad but still better than LCA.

A probable explanation for this that there is a spot in the seabottom with weak backscatter caused by low speckle. LCA choose weights steered towards this spot since it gives lower beam values. Therefore LCA get very low beam values and badly localized detections, since we have not removed low-amplitude detections. The uniform detections are much better since the bottom lie at almost

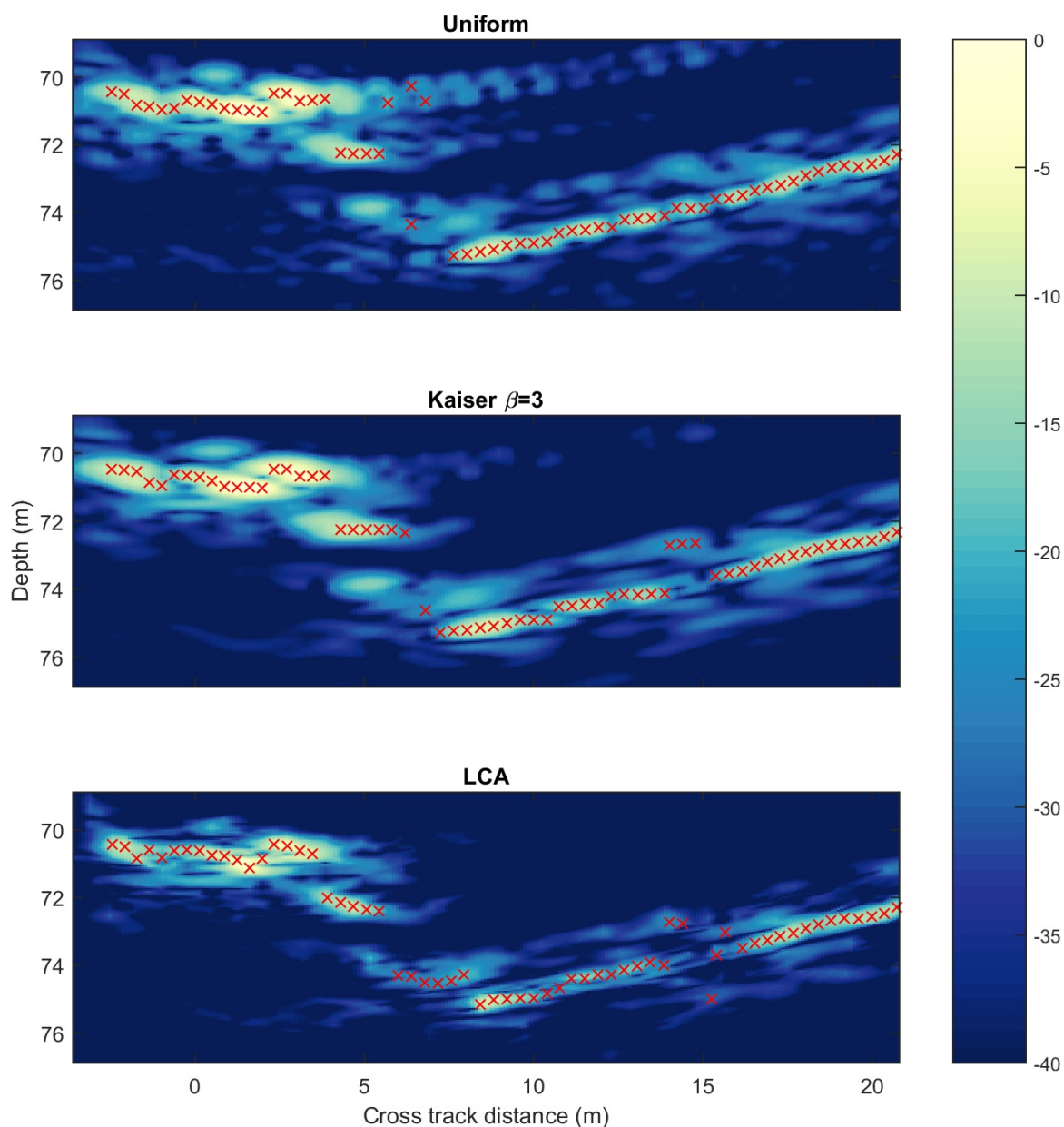


Figure 5: Beam power and bottom detections for different beamforming techniques on measured data, ping 69. Red crosses are amplitude detections. The colormap represent normalized beam power in dB. The strongest beam sample across the three beams is set to 0 dB.

constant range. Therefore, the weak spot is filled in by sidelobes and we coincidentally get good detections. The wide mainlobe of the kaiser weighted DAS make fill in the edges of the soft spot and give only one location for the misdetections. Therefore, the LCA image may represent the bottom better, although these detections should be discarded. A more sophisticated bottom detector would probably identify this as bad detections and then it will be a separate task to fill the gap.

The examples we have shown are extreme cases that represents the effects we see throughout the dataset. For example, the strong sidelobe arcs for the uniform beams are prevalent in most pings, but usually do not result in the amount of misdetections we saw in Figure 3.

5 CONCLUSIONS

Accurate mapping of the seabed using active high frequency sonar is of importance in many applications. In this paper we have considered three different beamformers: Uniformly weighted (or unweighted) DAS, kaiser weighted DAS and LCA. We have compared their performance on data collected by a seabed mapping echosounder of a scene containing a shipwreck. As in our previous work¹, LCA seem give the best performance.

Uniform DAS give high-resolution because a relatively narrow mainlobe but have high sidelobes, which give misdetections and false features in the water column plot. Kaiser weighted DAS avoid the misdetections with lower sidelobes but miss other features and smear out edges because of a wider mainlobe. LCA appear to simultaneously give better resolution than the uniform weighted DAS and better sidelobe suppression than kaiser weighted DAS. We see this as less sidelobes in the images, bottom detections that look more like a wreck contour and less like one beam dominating the neighbors, and smaller extension of localized targets.

LCA give worse detections in some low amplitude areas, while uniform and kaiser weights DAS seem to perform better. However, it seems likely that LCA still give a more representative image of the bottom, and that a more sophisticated detection algorithm would remove these detections.

Since we lack a true reference to verify this, these conclusions depend on our ability to guess the true structure of the scene. We feel that our interpretations are reasonable, but not infallible. Obtaining and comparing our result with high quality reference data is therefore a high priority for further work.

6 ACKNOWLEDGMENTS

We would like to thank Bente Borgundvåg Berg, Jan-Atle Storesund and Kjell Echholt Nilsen for their efforts. They have been vital for data collection, processing and analysis. The colormap used for the ping plots is based on a map from www.ColorBrewer.org.

This work is sponsored by The Research Council of Norway.

7 REFERENCES

1. T. I. B. Lønmo, A. Austeng, and R. E. Hansen, "Low complexity adaptive beamforming applied to sonar imaging (invited)," in *Proceedings of 3rd International Conference and Exhibition on Underwater Acoustics*, J. S. Papadakis and L. Bjørnø, Eds., Platania, Crete, Jun. 2015.
2. H. L. Van Trees, *Optimum array processing*, ser. Detection, Estimation, and Modulation Theory. Wiley-Interscience, 2002, vol. 4.
3. J. Synnevåg, A. Austeng, and S. Holm, "Adaptive beamforming applied to medical ultrasound imaging," *IEEE Transactions on Ultrasonics, Ferroelectrics, and Frequency Control*, vol. 54, no. 8, pp. 1606–1613, Aug. 2007.
4. —, "A low-complexity data-dependent beamformer," *IEEE Transactions on Ultrasonics, Ferroelectrics and Frequency Control*, vol. 58, no. 2, pp. 281–289, Feb. 2011.
5. A. Blomberg, A. Austeng, R. Hansen, and S. Synnes, "Improving sonar performance in shallow water using adaptive beamforming," *IEEE Journal of Oceanic Engineering*, vol. 38, no. 2, pp. 297–307, 2013.
6. J. I. Buskenes, A. Austeng, and C.-I. C. Nilsen, "A low complexity adaptive beamformer for active sonar imaging," in *Proceedings of the 4th International Conference & Exhibition on Underwater Acoustic Measurements: Technologies and Results*, J. S. Papadakis and L. Bjørnø, Eds., Greece, Jun. 2011, pp. 281–286.
7. X. Lurton, *An Introduction to Underwater Acoustics: Principles and Applications*, 2nd ed., ser. Springer Praxis Books. Springer, 2010.